

SUBMILLIMETER GALAXY NUMBER COUNTS AND MAGNIFICATION BY GALAXY CLUSTERS

MARCOS LIMA, BHUVNESH JAIN, MARK DEVLIN, AND JAMES AGUIRRE

Department of Physics & Astronomy, University of Pennsylvania, Philadelphia, PA 19104, USA; mlima@sas.upenn.edu

Received 2010 May 5; accepted 2010 May 18; published 2010 June 11

ABSTRACT

We present an analytical model that reproduces measured galaxy number counts from surveys in the wavelength range of $500\ \mu\text{m}$ – $2\ \text{mm}$. The model involves a single high-redshift galaxy population with a Schechter luminosity function that has been gravitationally lensed by galaxy clusters in the mass range 10^{13} – $10^{15}\ M_{\odot}$. This simple model reproduces both the low-flux and the high-flux end of the number counts reported by the BLAST, SCUBA, AzTEC, and South Pole Telescope (SPT) surveys. In particular, our model accounts for the most luminous galaxies detected by SPT as the result of high magnifications by galaxy clusters (magnification factors of 10–30). This interpretation implies that submillimeter (submm) and millimeter surveys of this population may prove to be a useful addition to ongoing cluster detection surveys. The model also implies that the bulk of submm galaxies detected at wavelengths larger than $500\ \mu\text{m}$ lie at redshifts greater than 2.

Key words: galaxies: clusters: general – gravitational lensing: strong – submillimeter: galaxies

Online-only material: color figures

1. INTRODUCTION

Over the last decade, submillimeter (submm) surveys have yielded significant advances in our understanding of the galaxy population responsible for the high-redshift component of the cosmic infrared background (CIB; Fixsen et al. 1996, 1998; Smail et al. 1997; Hughes et al. 1998; Barger et al. 1998; Dwek et al. 1998; Greve et al. 2004; Pope et al. 2006; Coppin et al. 2006; Devlin et al. 2009). With typical far-infrared (FIR) luminosities $>10^{12}\ L_{\odot}$, submm galaxies are presumed to be the high-redshift counterparts to (ultra)luminous infrared galaxies ((U)LIRGs). The high luminosity of these galaxies is the result of star formation rates of 100 – $1000\ M_{\odot}\ \text{yr}^{-1}$. Approximately half of these galaxies are located at $1.9 \lesssim z \lesssim 2.9$ (Chapman et al. 2005; Aretxaga et al. 2007), dominating the total star formation rate at this epoch (Pérez-González et al. 2005; Michałowski et al. 2009).

One way to express the results of submm surveys is through number counts of galaxies as a function of flux for each observed wavelength. The shape of these counts has been interpreted as arising from different populations of galaxies whose characteristics evolve over cosmic time (Lagache et al. 2003, 2004; Pearson & Khan 2009; Le Borgne et al. 2009). These empirical models have successfully reproduced the counts. However, they may be masking a simpler explanation for the departure of the counts from a Schechter distribution at the high-flux end: magnification due to high-redshift galaxy clusters and groups (e.g., Blain 1996; Perrotta et al. 2002; Negrello et al. 2007). In fact, the predictions of Perrotta et al. (2002) and Negrello et al. (2007) use the physical models of Granato et al. (2001, 2004), respectively, which explain the presence of a substantial high-redshift population prone to lensing effects.

Millimeter wavelength surveys have also aimed at detecting galaxy clusters via the Sunyaev Zel’dovich (SZ) effect (Hincks et al. 2008; Carlstrom et al. 2009); the first results, including cosmic microwave background power spectra and cluster catalogs, have been released recently (Fowler et al. 2010; Staniszewski et al. 2009; Vanderlinde et al. 2010).

The South Pole Telescope (SPT) has measured number counts of dusty galaxies at wavelengths $\lambda = 1.4\ \text{mm}$ and $2.0\ \text{mm}$ over

an area of $87\ \text{deg}^2$ (Vieira et al. 2009). The observed numbers at the bright end are higher than expected. The possibility that these galaxies lie at lower redshifts than the bulk of the population of submm galaxies is disfavored by the lack of detected counterparts in other surveys that probed the low- z population (Vieira et al. 2009). Placing these galaxies at high redshifts and assuming they are intrinsically bright would require them to be far more luminous than an underlying Schechter-like luminosity function would permit. Thus, the favored explanation is that they have typical luminosities for high- z galaxies, but have been magnified by foreground galaxies or clusters. In fact, lensing of high-redshift submm galaxies has been observed in a number of systems (Smail et al. 1997, 2002; Wilson et al. 2008; Rex et al. 2009; Gonzalez et al. 2009; Swinbank et al. 2010).

In this Letter, we explore the possibility that the existing observed galaxy number counts over a wide range of wavelengths can be reproduced by a *single* population of galaxies at high redshift. Foreground galaxy groups and clusters gravitationally lense the background submm population (Lima et al. 2009), leading to significant enhancements to the high-flux end of the galaxy counts. In Section 2, we describe the lensing magnification formalism, which we then apply to a high- z galaxy population and present results in Section 3. We discuss implications for high- z galaxies and cluster searches in Section 4.

Throughout, we use a flat cosmology with parameters based on the *Wilkinson Microwave Anisotropy Probe* (WMAP) fifth year data results (WMAP5; Komatsu et al. 2009). The cosmological parameters and their values are $\delta_{\zeta} = 2.41 \times 10^{-4}$ at $k = 0.02\ \text{Mpc}^{-1}$ (corresponding to $\sigma_8 = 0.8$), $n = 0.96$, $\Omega_b h^2 = 0.023$, $\Omega_m h^2 = 0.13$, $\Omega_{\text{DE}} = 0.74$, and $w = -1$. We also consider changes in σ_8 consistent with the WMAP5 errors of $\Delta\sigma_8 \approx 0.03$.

2. NUMBER COUNTS WITH LENSING MAGNIFICATION

In recent papers (Lima et al. 2009; Jain & Lima 2010), we have presented a halo model for calculating the effects of lensing magnification by galaxy groups and clusters. Here, we specialize to the case of steep galaxy counts at high redshifts, where lensing effects are quite dramatic. We assume a Schechter function

(Schechter 1976) for the intrinsic number density distribution of a population of galaxies:

$$\frac{dn}{dS} = \frac{n^*}{S^*} \left(\frac{S}{S^*} \right)^\alpha e^{-S/S^*}, \quad (1)$$

where n^* , S^* , and α are free parameters. Lensing magnification by intervening halos changes the intrinsic dn/dS to its observed counterpart as

$$\frac{dn_{\text{obs}}(S_{\text{obs}})}{dS_{\text{obs}}} = \int d\mu \frac{P(\mu)}{\mu} \frac{dn}{dS} \left(\frac{S_{\text{obs}}}{\mu} \right), \quad (2)$$

where μ is the lensing magnification and $P(\mu)$ is its probability for a given galaxy population at redshift z_s . Conditional probabilities quantify the effects of different magnification ranges on the observed flux density S_{obs} . The integrand of Equation (2) defines the probability $P(\mu|S_{\text{obs}})$:

$$P(\mu|S_{\text{obs}}) = \left(\frac{dn_{\text{obs}}(S_{\text{obs}})}{dS_{\text{obs}}} \right)^{-1} \frac{P(\mu)}{\mu} \frac{dn}{dS} \left(\frac{S_{\text{obs}}}{\mu} \right), \quad (3)$$

which can be interpreted as the relative contribution of a given μ to the total $dn_{\text{obs}}/dS_{\text{obs}}$ at S_{obs} (Paciga et al. 2009). Similarly, $P(\mu_{\text{min}}|S_{\text{obs}}) = \int_{\mu_{\text{min}}}^{\infty} d\mu P(\mu|S_{\text{obs}})$ measures the integrated contribution from all $\mu > \mu_{\text{min}}$. The mean magnification at a given S_{obs} is defined as

$$\langle \mu \rangle (S_{\text{obs}}) = \int_0^{\infty} d\mu \mu P(\mu|S_{\text{obs}}). \quad (4)$$

The distribution $P(\mu)$ can be estimated either by ray-tracing on N -body simulations (e.g., Hilbert et al. 2007), or by semi-analytical methods (e.g., Perrotta et al. 2002; Lima et al. 2009), integrating halo contributions on the line of sight up to the source redshift:

$$P(> \mu) = \int_0^{z_s} dz_l \frac{D_A^2(z_l)}{H(z_l)} \int_{M_{\text{th}}}^{\infty} d \ln M \frac{dn(z_l, M)}{d \ln M} \Delta\Omega_\mu, \quad (5)$$

where D_A is the angular diameter distance, H is the Hubble parameter, $dn/d \ln M$ is the halo mass-function, and $\Delta\Omega_\mu = \Delta\Omega_\mu(z_s, z_l, M)$ is the cross-section for magnifications larger than μ produced by halos of mass M at redshift z_l on sources at redshift z_s . The integrand,

$$\frac{d^2 P(> \mu)}{d \ln M dz_l} = \frac{D_A^2(z_l)}{H(z_l)} \frac{dn(z_l, M)}{d \ln M} \Delta\Omega_\mu, \quad (6)$$

gives the range of halo masses and redshifts contributing to the probability of a minimum magnification μ .

In summary, Equations (2) and (5) give the total effect on the counts, Equation (3) indicates which magnifications contribute most to a given S_{obs} , and Equation (6) tells us which halo masses and redshifts contribute to a given magnification.

We use this halo-model $P(\mu)$ and correct it for a number of effects. First, as described in Lima et al. (2009), we match our $P(\mu)$ at large magnifications to that of ray-tracing in dark matter simulations (Hilbert et al. 2007) by tuning the ellipticity of our halos. Next, we account for the effect of luminous matter, which can lead to higher densities via gas cooling, using the simulation results of Hilbert et al. (2008). We also correct for

the combination of finite source size and multiple image effects. Finally, magnification effects are sensitive to the value of σ_8 since it affects the abundance of cluster halos. In the next section, we discuss how we account for the uncertainties in our model by giving a range for our predictions.

Our analytical calculation of $P(\mu)$ has some advantages over the approach of numerical simulations (we can easily study changes in source redshift, σ_8 , and the contribution from different halo masses and redshift), but it also has limitations. We only use the one-halo term, which is accurate at the high magnifications relevant for the effects considered here but overestimates the lensing contribution at $\mu \sim 1$. We do not include a distribution of ellipticities or halo substructure, which can also increase magnification cross-sections. We have instead tuned the average halo ellipticity to match the $P(\mu)$ measured in dark matter simulations (see Lima et al. 2009 for a detailed discussion). And whereas we account for the effects of baryons observed in simulations by Hilbert et al. (2008), these authors note that their results still underestimate baryonic effects for halos of smaller masses as they do not predict sufficient numbers of multiple-imaged quasars. Finally, the effect of finite source size is very uncertain given the lack of our knowledge about submm galaxies and the sensitivity to the precise caustic structure of the lenses (e.g., Li et al. (2005). Proper inclusion of all these missing effects would likely increase the magnification probabilities compared with our current model.

3. RESULTS

In Figure 1, we illustrate the lensing effect on an intrinsic Schechter distribution given by Equation (1) for sources at different redshifts. In all our results, we fix $\alpha = -1.0$ and $n^* = 5 \times 10^3 \text{ deg}^{-2}$. Changing to $\alpha = -1.5$ does not have a significant effect; while it matches the faint end behavior of dn/dS for the model of Lagache et al. (2004), we preferred to use $\alpha = -1.0$ since this better fits the number counts at shorter wavelengths. With these parameter values, our counts are lower than the model of Lagache et al. (2004) at all S , which also ensures that the total flux does not exceed the CIB (Dwek et al. 1998).

Figure 2 illustrates our main results: we show predicted number counts that include lensing (gray bands), assuming galaxies at $z_s = 3.0$, along with measured number counts from submm surveys at different wavelengths. As indicated in the panels, these are BLAST at $\lambda = 500 \mu\text{m}$ (Devlin et al. 2009), SCUBA at $\lambda = 850 \mu\text{m}$ (Coppin et al. 2006), AzTEC at 1.1 mm (Austermann et al. 2010), and SPT *dusty* submm galaxies at $\lambda = 1.4 \text{ mm}$ and 2.0 mm (Vieira et al. 2009). In all of our results, the SPT number counts correspond to those of Vieira et al. (2009), after removing both synchrotron emission galaxies as well as low-redshift galaxies that have matches with galaxies in the *Infrared Astronomy Satellite* (IRAS) survey (Moshir et al. 1992; Fisher et al. 1995; Oliver et al. 1996). Predictions are shown by bands rather than curves to reflect the uncertainties in the model as discussed below. All the data sets can be fit by changing the single parameter S^* once lensing magnification is included. This remarkable result implies that, within the measurement and theoretical uncertainties, a single high- z population of galaxies is sufficient to describe all the observations. The high-flux measurements of BLAST and SPT are fit by highly magnified galaxies—if these counts were dominated by a population of a different galaxy type, it would be a coincidence that their relative counts fit the same scaling with wavelength as the fainter (normal) population. Finally, we

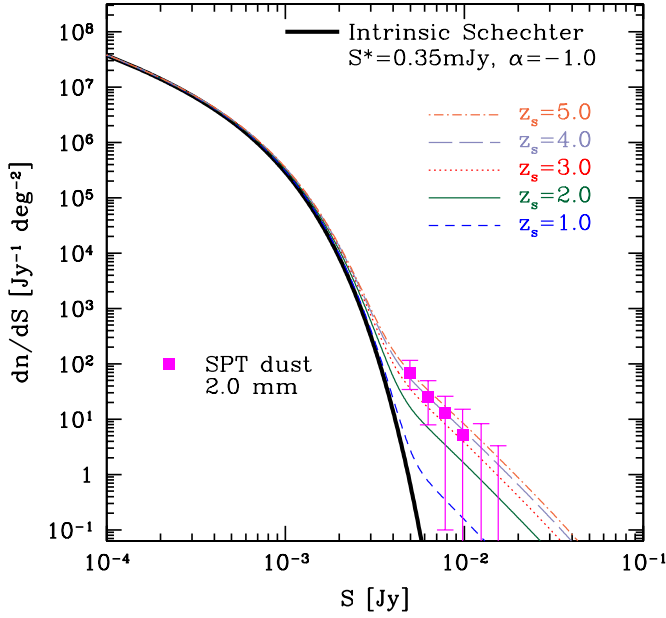


Figure 1. Intrinsic and lensed number counts dn/dS for a Schechter function describing galaxies at different redshifts. Also shown are the observed counts for SPT *dusty* submm galaxies at $\lambda = 2.0$ mm, after removal of low-redshift galaxies with *IRAS* counterparts.

(A color version of this figure is available in the online journal.)

also show a prediction for MUSTANG at 3.3 mm (Mason et al. 2006), which has begun operating on the Green Bank Telescope.

The lower bound for the predictions in Figure 2 uses $\sigma_8 = 0.77$, while the upper bound uses $\sigma_8 = 0.83$ —these reflect the uncertainties in the WMAP5 results. The enhancement due to baryons is factored into these predictions, though it is likely to be an underestimate as discussed in Section 2. The effect of source sizes and multiple imaging is uncertain; we simply assume that, due to the finite source size, the effective

magnification is reduced by 50%–25% (for the lower and upper bounds, respectively)

The right panel of Figure 2 shows all points rescaled by plotting

$$\frac{d\tilde{n}}{d\tilde{S}} = \tilde{S}^\alpha e^{-\tilde{S}}, \quad (7)$$

where $\tilde{n} = n/n^*$ and $\tilde{S} = S/S^*$. In Figure 3, we show values of S^* used for each wavelength. We compared the frequency scaling of S^* with that of a typical spectral energy distribution (SED) of submm galaxies $SED(\lambda) \propto \epsilon(\lambda)B(T, \lambda)$, redshifted to $z_s = 3$ with emissivity $\epsilon(\lambda) = 1 - \exp[-(\lambda_0/\lambda)^\beta]$ and blackbody spectrum $B(T, \lambda)$ at temperature T . The values of S^* are consistent with $\beta = 1$ –2 and $T = 30$ –40 K.

The fit to the BLAST counts at $\lambda = 500, 350,$ and $250 \mu\text{m}$ falls further below the high-flux measurement at shorter wavelengths, suggesting the need for a lower redshift population. Indeed, Eales et al. (2009) have identified the radio and $24 \mu\text{m}$ counterparts of the bright BLAST sources. Almost all of the bright sources at $250 \mu\text{m}$, and one third to one half of the sources in the highest flux bin at $500 \mu\text{m}$ are identified as being at $z < 1$. Removing these would lower the corresponding point in Figure 2, in agreement with the model. The remaining sources at $500 \mu\text{m}$ (and less than a tenth of the sources at $250 \mu\text{m}$) are likely the result of lensing. Similar results should be expected with the upcoming release of the large-area Herschel surveys.

Since the lensed distributions at $z_s = 3.0$ are consistent with SPT data points at both wavelengths, we study the range of magnifications and halo masses that contribute most in this case. As we consider $S_{\text{obs}}/S^* \gtrsim 10$, the observed sources come from intrinsically low-flux sources which have been significantly magnified. Figure 4 shows $P(\mu_{\text{min}}|S_{\text{obs}})$ and $\langle \mu \rangle$ as a function of S_{obs} for SPT ($\lambda = 1.4$ mm) and indicates magnifications that contribute the most at each S_{obs} . For instance, for $S_{\text{obs}} = 20$ –40 mJy, $\langle \mu \rangle \sim 20$ –30, and $P(\mu_{\text{min}}|S_{\text{obs}}) > 0.5$ for $\mu_{\text{min}} \sim 10$ –20.

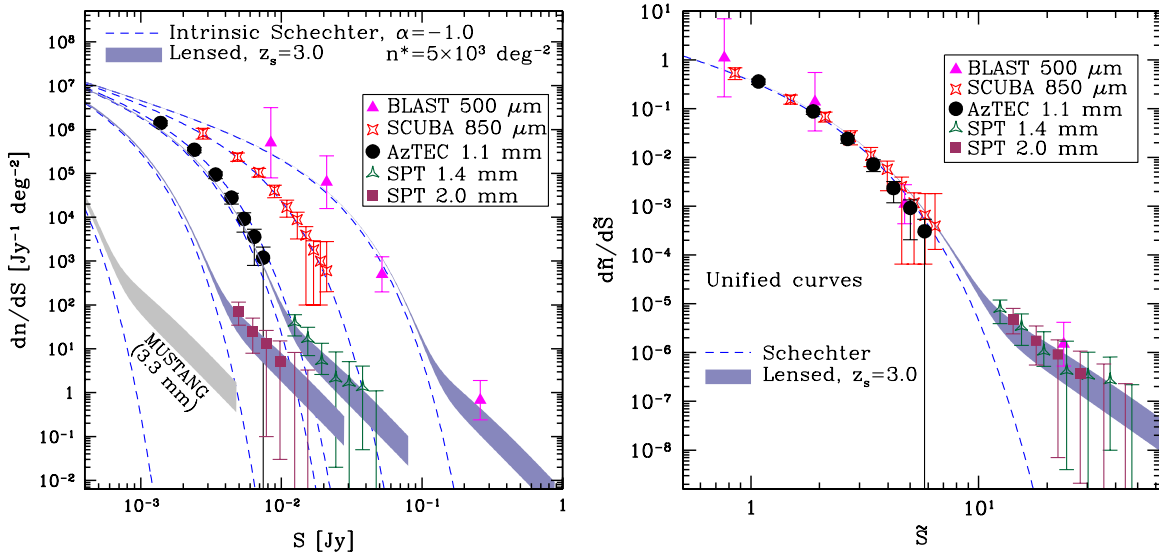


Figure 2. Left : intrinsic and lensed dn/dS for a Schechter function describing galaxies at $z_s = 3.0$ and different wavelengths. Dashed lines indicate the intrinsic Schechter functions (with different S^* values), and the dark shaded regions display the range of lensing predictions, as described in the text. Also shown are observed counts for BLAST at $\lambda = 500 \mu\text{m}$, SCUBA at $\lambda = 850 \mu\text{m}$, AzTEC at $\lambda = 1.1$ mm, and SPT at both $\lambda = 1.4$ mm and 2.0 mm. The SPT counts are for *dusty* galaxies, after removal of galaxies with *IRAS* counterparts. No similar removal has been applied to the BLAST data, which includes both high- and low-redshift galaxies. Notice that we do not display lensing predictions for SCUBA and AzTEC. A prediction for MUSTANG at $\lambda = 3.3$ mm is shown in the light-shaded region. Right : unified rescaled curves showing $d\tilde{n}/d\tilde{S}$ and the various data points. The only parameter used in the scaling is S^* (see Figure 3).

(A color version of this figure is available in the online journal.)

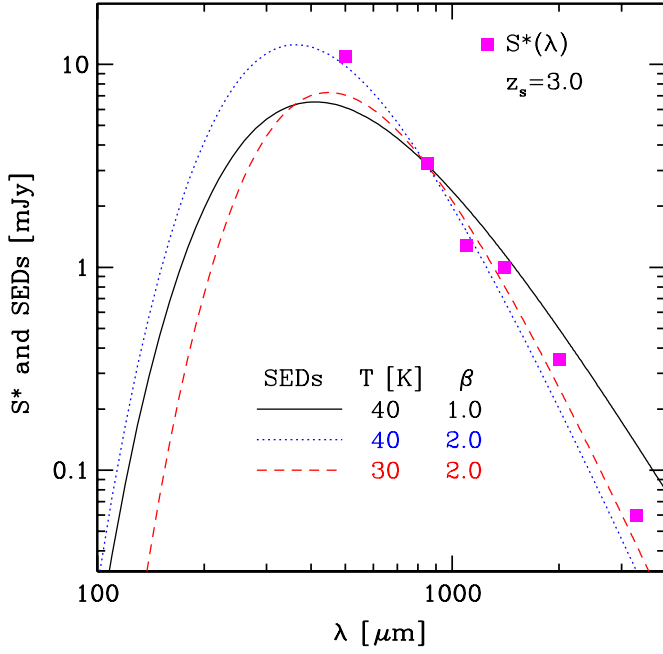


Figure 3. Flux scale S^* in the Schechter function for various surveys at different wavelengths (symbols). The three curves show the expected scaling for submm galaxy SEDs at $z_s = 3.0$ for different values of spectral index β and temperature T . The curves are normalized at the value of S^* for $\lambda = 850 \mu\text{m}$.

(A color version of this figure is available in the online journal.)

These results imply that magnifications of 10–30 are necessary to explain the boost in dn/dS at $S_{\text{obs}} \sim 10\text{--}40$ mJy, if it is due to lensing of an intrinsic Schechter distribution. Note that due to the finite size of submm galaxies, their magnifications must have a cutoff, which has been estimated to be in the range $\mu \sim 10\text{--}40$ (Perrotta et al. 2002) for galaxy lenses, and is probably a factor of 2 or so larger for more massive lenses. Indeed, galaxies have been measured with estimated magnifications of at least ~ 45 (Kneib et al. 2004).

In Figure 5, we show $d^2P/d \ln M dz_l$ as a function of halo mass for different values of μ_{min} and z_l . This indicates

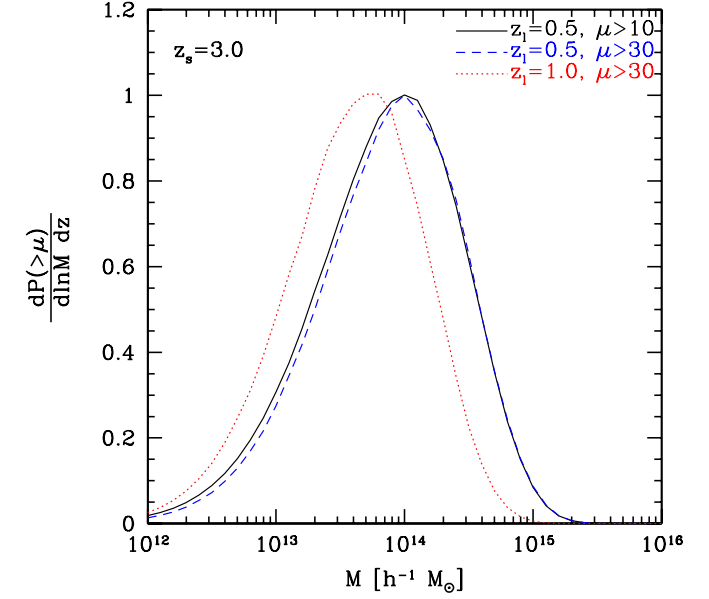
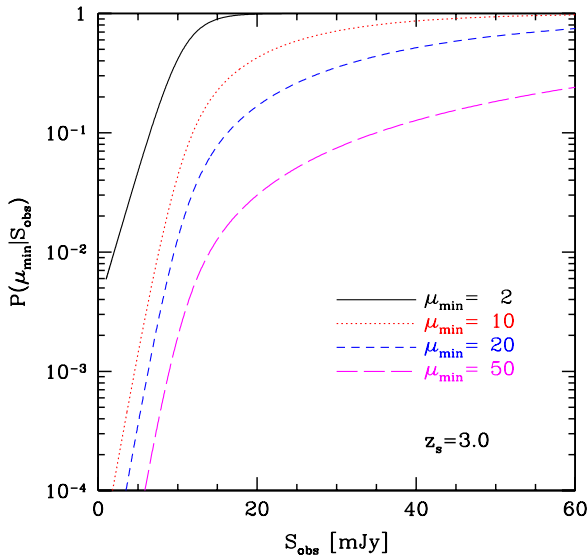


Figure 5. Integrand $d^2P(> \mu)/d \ln M dz_l$ as a function of halo mass M for different values of μ and z_l . We have arbitrarily normalized these curves for better visualization. Note that the peak lensing contribution for source galaxies at $z_s = 3$ comes from lens halos at $z_l \sim 0.5$. This does not include baryonic effects, which boost the contribution from $M \lesssim 10^{13} h^{-1} M_\odot$ halos.

(A color version of this figure is available in the online journal.)

that halo masses above $10^{13} h^{-1} M_\odot$ contribute significantly to magnifications of 10–30, with most of the contribution coming from $\sim 10^{14} h^{-1} M_\odot$. Note that this does not include baryonic effects, which boost the contribution from lower mass ($\lesssim 10^{13} h^{-1} M_\odot$) halos as discussed in Section 2.

We have assumed that all source galaxies are at a fixed redshift z_s , whereas in reality they have a redshift distribution which needs to be incorporated in the computation. The curves at different source redshifts shown in Figure 1 provide approximate limits for what we can expect from a redshift distribution of source galaxies. Our results imply that the bulk of the

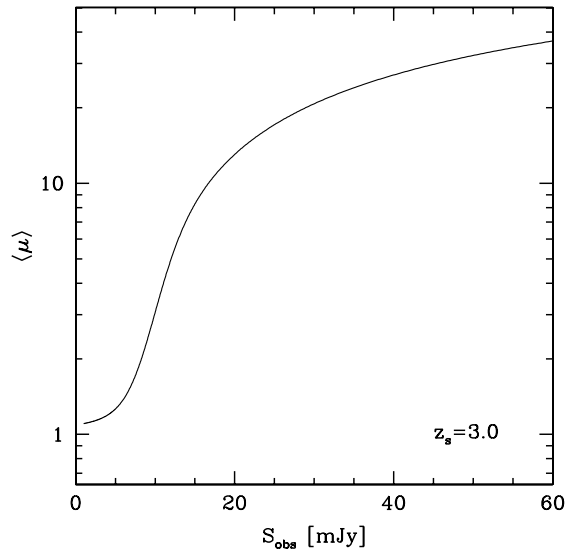


Figure 4. Probability $P(\mu_{\text{min}}|S_{\text{obs}})$ of the minimum magnification μ_{min} , given an observed flux density S_{obs} (left panel), and the corresponding average magnification $\langle \mu \rangle$ (right panel). We assume a Schechter function describing galaxies at $z_s = 3.0$ which, after lensing, predicts counts consistent with those of SPT dusty submm galaxies at $\lambda = 1.4$ mm (see Figure 2).

(A color version of this figure is available in the online journal.)

population of submm galaxies is at redshifts $z \gtrsim 2$. The alternative explanation for the high-flux measurements is to have a significant fraction of galaxies at very low z , which would easily have been observed in surveys such as *IRAS* (indeed, the SPT data shown remove the small fraction of such sources). As shown in Figure 1, galaxies at higher redshift but still at $z \lesssim 1$ would not match the measurements as the magnification boost is insufficient (again within the context of an underlying Schechter distribution).

4. DISCUSSION

We have considered the possibility that bright millimeter and submm galaxy counts arise largely from a galaxy population at high redshifts that is lensed by intervening galaxy groups and clusters. Our model predictions match the counts from 500 μm to 2 mm from the BLAST, SCUBA, AzTEC, and SPT surveys (see Figure 2). We find that the high-flux SPT number counts can be explained by highly magnified galaxies from this high- z population (once the known, low- z counterparts detected in *IRAS* are removed). This high- z galaxy population is described by a Schechter luminosity function with $L^* \sim 2.5 \times 10^{12} L_\odot$ and a source redshift $z_s = 3.0$. Our model predictions fit the data for $500\mu\text{m} < \lambda < 2\text{mm}$ by varying S^* with wavelength within the range of typical submm galaxy SEDs (see Figure 3).

Our model has some simplifying assumptions, such as the fixed source redshift $z_s = 3$, and there are significant measurement and theoretical uncertainties. A complete analysis would require a more detailed treatment of lensing effects and inclusion of the measured galaxy clustering. In addition, it has been established that at the shorter wavelengths probed by BLAST, an increasing fraction of sources lie at low- z —hence, we can expect a smooth variation in the fraction of low- z galaxies with observed wavelength.

Nevertheless, our results in Figure 2 imply that current number counts do not require an additional galaxy population to explain the high-flux measurements. Such a population has been invoked in theoretical models (e.g., Lagache et al. 2003) and suggested as a possible explanation (as well as lensing of the high- z population) for the recent SPT measurements (Vieira et al. 2009). Indeed, adding a significant fraction of a second population could cause the predictions to exceed the measured counts once magnification effects for the high- z population are included. It would also be difficult to explain how the scaling with wavelength of the high-flux number counts is the same as the lower flux counts if they came from different galaxy populations. Since lensing does not depend on frequency, our model naturally follows this common scaling.

Current SZ surveys with sensitivities of $(3\text{--}7) \times 10^{14} h^{-1} M_\odot$ cannot detect most halos that produce this lensing contribution. Conversely, looking for extremely bright objects in millimeter and submm wavelengths provides a way to find high- z lensing halos associated with galaxy groups and clusters. The number of halos that can be found in this way is only a small fraction of all halos within a given mass range. As discussed above, our model most likely underestimates the contribution from halos with $M \lesssim 10^{13} M_\odot$. It is therefore of great interest to investigate the lenses corresponding to the bright sources in current data.

Follow-up observations with optical telescopes should be able to identify lensing group/cluster candidates up to $z \simeq 1$. These clusters and groups host the brightest cluster galaxies with luminosities $L \sim 10^{11}\text{--}10^{12} L_\odot$, based on the low- z results of Johnston et al. (2007). Multi-band optical imaging with limiting magnitude of 23–24 (for the r band) would enable

identification of these groups and clusters. Conversely, targeted observations of the high magnification regions of known strong lensing clusters could provide detections of faint submm galaxies (which would lie below the detection threshold without the magnification boost). Similar to the use of clusters as gravitational telescopes in optical imaging, this may also help resolve submm galaxies. Planned observations with AzTEC and the Large Millimeter Telescope have considered such an approach (D. Hughes 2010, private communication).

We thank David Hughes, Roxana Lupu, Joaquin Vieira, Kim Scott, Ian Smail, Eric Switzer, and various members of the ACT collaboration for useful discussions. We benefited from discussions on strong lensing effects with Matthias Bartelmann, Gary Bernstein, Neal Dalal, and Ravi Sheth. We are very grateful to Stefan Hilbert for sharing his simulation results and Eric Switzer for providing the SPT data. This work was supported in part by an NSF-PIRE grant and AST-0607667.

REFERENCES

- Aretxaga, I., et al. 2007, *MNRAS*, **379**, 1571
Austermann, J. E., et al. 2010, *MNRAS*, **401**, 160
Barger, A. J., Cowie, L. L., Sanders, D. B., Fulton, E., Taniguchi, Y., Sato, Y., Kawara, K., & Okuda, H. 1998, *Nature*, **394**, 248
Blain, A. W. 1996, *MNRAS*, **283**, 1340
Carlstrom, J. E., et al. 2009, arXiv:0907.4445
Chapman, S. C., Blain, A. W., Smail, I., & Ivison, R. J. 2005, *ApJ*, **622**, 772
Coppin, K., et al. 2006, *MNRAS*, **372**, 1621
Devlin, M. J., et al. 2009, *Nature*, **458**, 737
Dwek, E., et al. 1998, *ApJ*, **508**, 106
Eales, S., et al. 2009, *ApJ*, **707**, 1779
Fisher, K. B., Huchra, J. P., Strauss, M. A., Davis, M., Yahil, A., & Schlegel, D. 1995, *ApJS*, **100**, 69
Fixsen, D. J., Cheng, E. S., Gales, J. M., Mather, J. C., Shafer, R. A., & Wright, E. L. 1996, *ApJ*, **473**, 576
Fixsen, D. J., Dwek, E., Mather, J. C., Bennett, C. L., & Shafer, R. A. 1998, *ApJ*, **508**, 123
Fowler, J. W., et al. 2010, arXiv:1001.2934
Gonzalez, A. H., Clowe, D., Bradač, M., Zaritsky, D., Jones, C., & Markevitch, M. 2009, *ApJ*, **691**, 525
Granato, G. L., De Zotti, G., Silva, L., Bressan, A., & Danese, L. 2004, *ApJ*, **600**, 580
Granato, G. L., Silva, L., Monaco, P., Panuzzo, P., Salucci, P., De Zotti, G., & Danese, L. 2001, *MNRAS*, **324**, 757
Greve, T. R., Ivison, R. J., Bertoldi, F., Stevens, J. A., Dunlop, J. S., Lutz, D., & Carilli, C. L. 2004, *MNRAS*, **354**, 779
Hilbert, S., White, S. D. M., Hartlap, J., & Schneider, P. 2007, *MNRAS*, **382**, 121
Hilbert, S., White, S. D. M., Hartlap, J., & Schneider, P. 2008, *MNRAS*, **386**, 1845
Hincks, A. D., et al. 2008, Proc. SPIE, 7020, 1
Hughes, D. H., et al. 1998, *Nature*, **394**, 241
Jain, B., & Lima, M. 2010, arXiv:1003.6127
Johnston, D. E., et al. 2007, arXiv:0709.1159
Kneib, J., van der Werf, P. P., Kraiberg Knudsen, K., Smail, I., Blain, A., Frayer, D., Barnard, V., & Ivison, R. 2004, *MNRAS*, **349**, 1211
Komatsu, E., et al. 2009, *ApJS*, **180**, 330
Lagache, G., Dole, H., & Puget, J. 2003, *MNRAS*, **338**, 555
Lagache, G., et al. 2004, *ApJS*, **154**, 112
Le Borgne, D., Elbaz, D., Ocvirk, P., & Pichon, C. 2009, *A&A*, **504**, 727
Li, G., Mao, S., Jing, Y. P., Bartelmann, M., Kang, X., & Meneghetti, M. 2005, *ApJ*, **635**, 795
Lima, M., Jain, B., & Devlin, M. 2009, arXiv:0907.4387
Mason, B. S., Dicker, S., Korngut, P., Benford, D., Devlin, M., Irwin, K., Moseley, H., & MUSTANG Collaboration 2006, *BAAS*, **38**, 1015
Michałowski, M. J., Hjorth, J., & Watson, D. 2010, *A&A*, **514**, A67
Moshir, M., Kopman, G., & Conrow, T. A. O. 1992, *IRAS Faint Source Survey, Explanatory Supplement Version 2*, ed. M. Moshir, G. Kopman, & T. A. O. Conrow (Pasadena, CA: Infrared Processing and Analysis Center, California Institute of Technology)

- Negrello, M., Perrotta, F., González-Nuevo, J., Silva, L., de Zotti, G., Granato, G. L., Baccigalupi, C., & Danese, L. 2007, *MNRAS*, 377, 1557
- Oliver, S. J., et al. 1996, *MNRAS*, 280, 673
- Paciga, G., Scott, D., & Chapin, E. L. 2009, *MNRAS*, 395, 1153
- Pearson, C., & Khan, S. A. 2009, *MNRAS*, 399, L11
- Pérez-González, P. G., et al. 2005, *ApJ*, 630, 82
- Perrotta, F., Baccigalupi, C., Bartelmann, M., De Zotti, G., & Granato, G. L. 2002, *MNRAS*, 329, 445
- Pope, A., et al. 2006, *MNRAS*, 370, 1185
- Rex, M., et al. 2009, *ApJ*, 703, 348
- Schechter, P. 1976, *ApJ*, 203, 297
- Smail, I., Ivison, R. J., & Blain, A. W. 1997, *ApJ*, 490, L5
- Smail, I., Ivison, R. J., Blain, A. W., & Kneib, J. 2002, *MNRAS*, 331, 495
- Staniszewski, Z., et al. 2009, *ApJ*, 701, 32
- Swinbank, M., et al. 2010, *Nature*, 464, 733
- Vanderlinde, K., et al. 2010, arXiv:1003.0003
- Vieira, J. D., et al. 2009, arXiv:0912.2338
- Wilson, G. W., et al. 2008, *MNRAS*, 390, 1061